Expanded View Figures

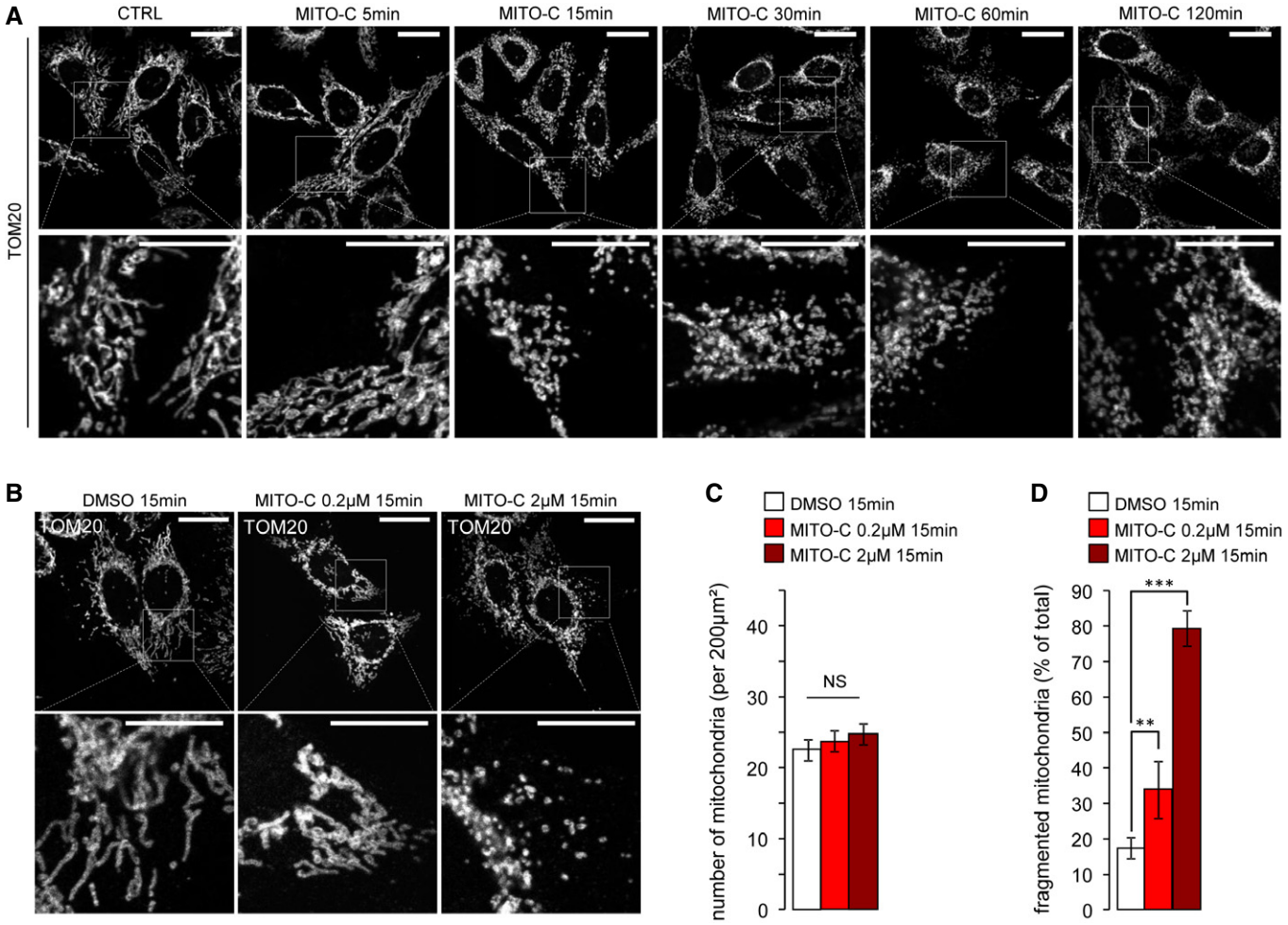

Figure EV1. Time- and dose-dependent mitochondrial fragmentation induced by Mito-C.

A HeLa cells were treated with 2 µM Mito-C for the indicated times, fixed and immunostained for TOM20, and analyzed by light microscopy.

B HeLa cells were treated with increasing concentrations of Mito-C for 15 min, fixed and immunostained for TOM20, and analyzed by light microscopy.

C Quantification of mitochondria number (based on TOM20 immunostaining as shown in B, $n = 30$). Errors bars show the standard error of the mean (SEM).

D Quantification of mitochondria phenotype morphology (based on TOM20 immunostaining as shown in B, $n = 45$–50). Errors bars show the standard error of the mean (SEM).

Data information: To evaluate significance of differences observed in C, one-way ANOVA followed by Bonferroni's post-test was used (** indicates $P < 0.001$ and ***$P < 0.0001$). Scale bars = 10 µm, except 5 µm in magnification areas in A and B.

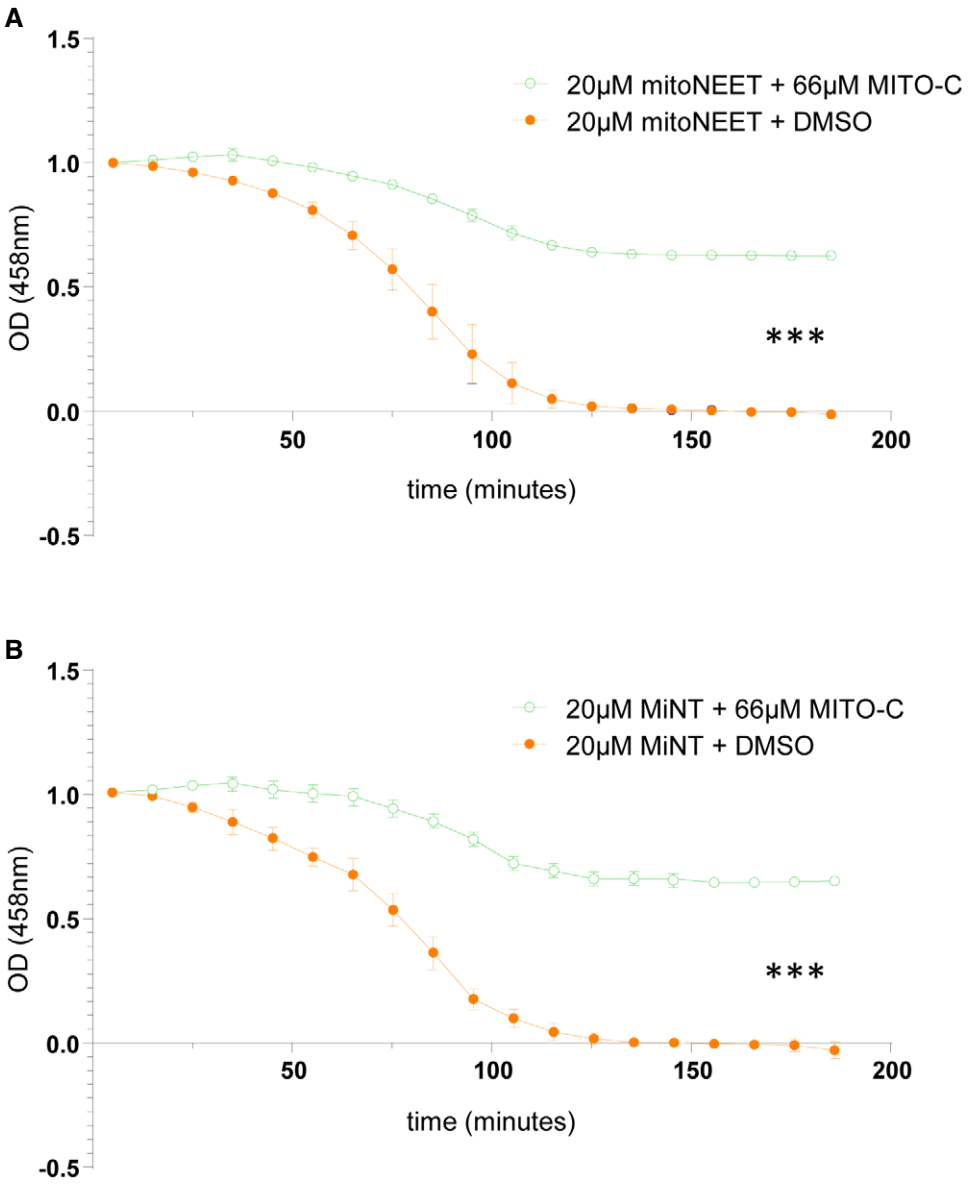

Figure EV2. Mito-C impacts Fe-S clusters release from MitoNEET and MiNT proteins.

A, B Profile of [2Fe–2S] clusters release from purified recombinant MitoNEET and MiNT were determined in presence or absence (DMSO) of Mito-C via monitoring their absorbance at 458 nm as a function of time. Errors bars show the standard deviation (SD) of 3 independent experiments.

Data information: For differences observed in both A and B, one-way ANOVA followed by Dunn's post-test was used ($N = 3$, *** indicates $P < 0.0001$).

Figure EV3. Mitochondrial characteristics of Mito-C treated cells.

A HeLa cells were treated with 2 μM Mito-C or DMSO for 24 h. Cells were fixed and prepared for electron microscopy analyses (left panel). Intact mitochondrial cristae were quantified (right panel). Errors bars show the standard deviation (SD) of 3 independent experiments.

B Oxygen consumption rate (OCR) of cells treated with Mito-C (2, 10 and 20μM) were measured by Seahorse© technique. Measurements start before starting the treatment, arrow indicates the Mito-C injection. Graphs show the standard deviation (SD) of 3 independent experiments.

C To evaluate the mitochondrial potential, cells were treated with Mito-C for 24 h at the indicated range of concentrations and stained with MitoTracker Redox and analyzed by cytometry. Graphs show the standard deviation (SD) of 3 independent experiments.

D To evaluate the mitochondrial potential, cells were treated with Mito-C at 2 μM over a time course and then stained with MitoTracker Redox and analyzed by cytometry. Graphs show the standard deviation (SD) of 3 independent experiments.

E To evaluate the total mitochondrial mass over a time course of treatment, HeLa cells were treated with DMSO or Mito-C at 2 μM for the time duration indicated, stained with MitoTracker green and analyzed by cytometry. Graphs show the standard deviation (SD) of 3 independent experiments.

F To evaluate the total mitochondrial mass at a fixed time point following treatment with an increasing range of concentrations of Mito-C cells were treated with DMSO or Mito-C for 24 h at concentration indicated, stained with MitoTracker green and analyzed by cytometry. Graphs show the standard deviation (SD) of 3 independent experiments.

G High-resolution respirometry (HRR) evaluation of HeLa cells treated for 15 min with 2 μM Mito-C. Different bioenergetics parameters were analyzed: routine respiration, oligomycin-sensitive, and CCCP-sensitive. The term "routine" respiration is defined as the respiratory rate of intact cells measured in 5 mM glucose DMEM under atmospheric conditions at 37°C and sensitive to 2.5 μM antimycin A inhibition. The term "oligo insensitive" respiration is the respiratory rate measured in the routine conditions after addition of the F1F0-ATP synthase inhibitor oligomycin at 20 μg/ml. This "oligomycin" state of respiration does not depend on ADP phosphorylation. The ATP-linked respiration is calculated as the difference between the routine and the oligomycin-sensitive. The term "uncoupled" respiration defines the rate of respiration measured in the "oligo" conditions after addition of the uncoupler CCCP used at 2 μM. The "CCCP" state allows evaluating the maximal capacity of the respiratory chain in presence of energy substrates and oxygen concentration as defined in the "routine" conditions. The ATP-linked respiration (routine-oligo) indicates the part of respiration used for ATP synthesis and the spare respiratory capacity (CCCP-routine) gives a measure of the capacity of the respiratory chain to be chemically uncoupled. It indicates how far from the maximal capacity the routine respiration operates. Bars show the standard deviation (SD) of 3 independent experiments.

H Comparison of cell viability from HeLa cells grown on high glucose (25 mM) (open bar) versus cells grown on galactose (10 mM) (solid bar) treated with 2 μM Mito-C for 24 h. Data are expressed as mean ± SEM of $N = 3$ biological replicates.

Data information: For evaluating significance of differences observed in A, *t*-test was used (*** indicates $P < 0.0001$). Scale bar in A = 200 nm.

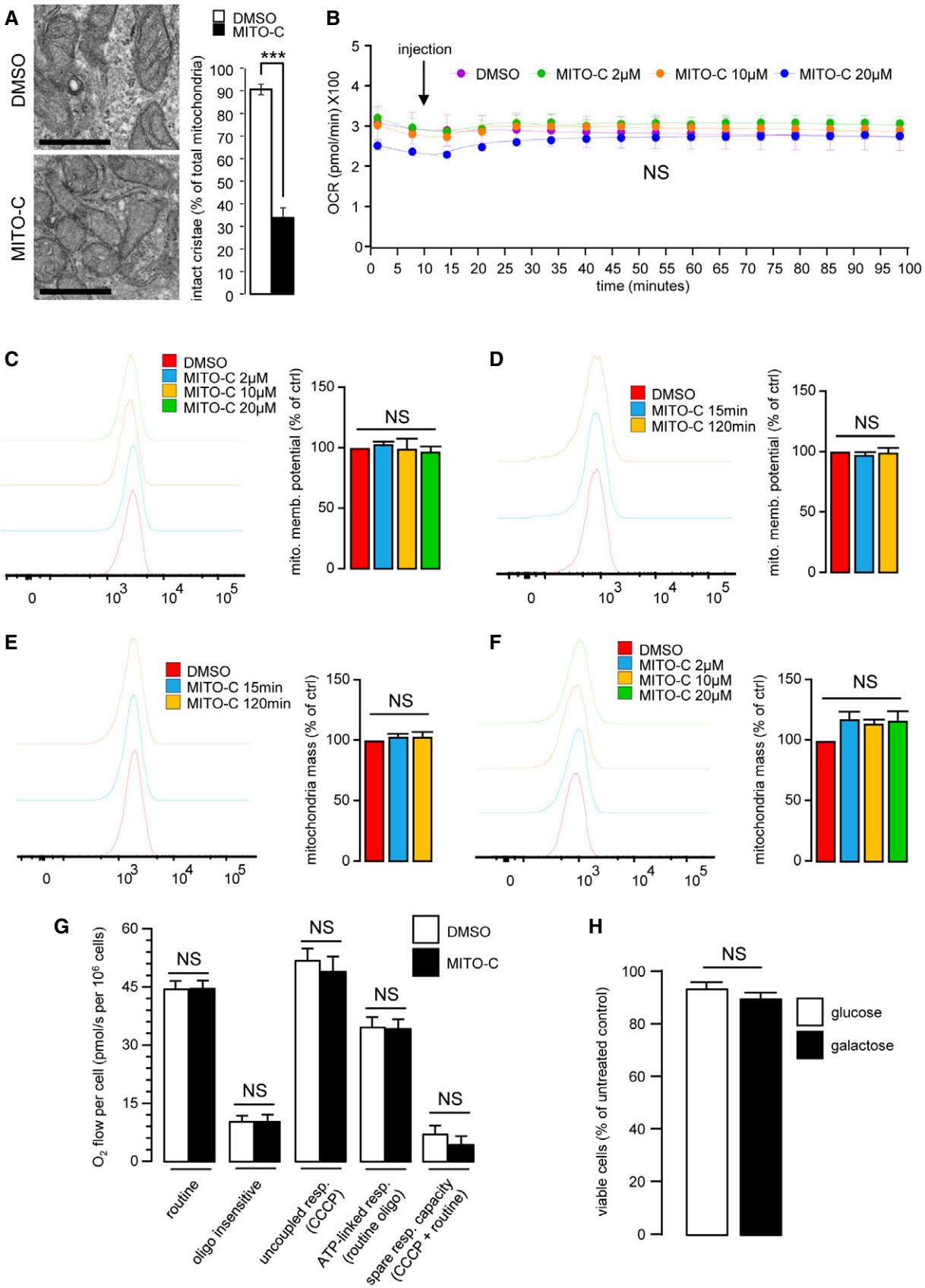

Figure EV3.

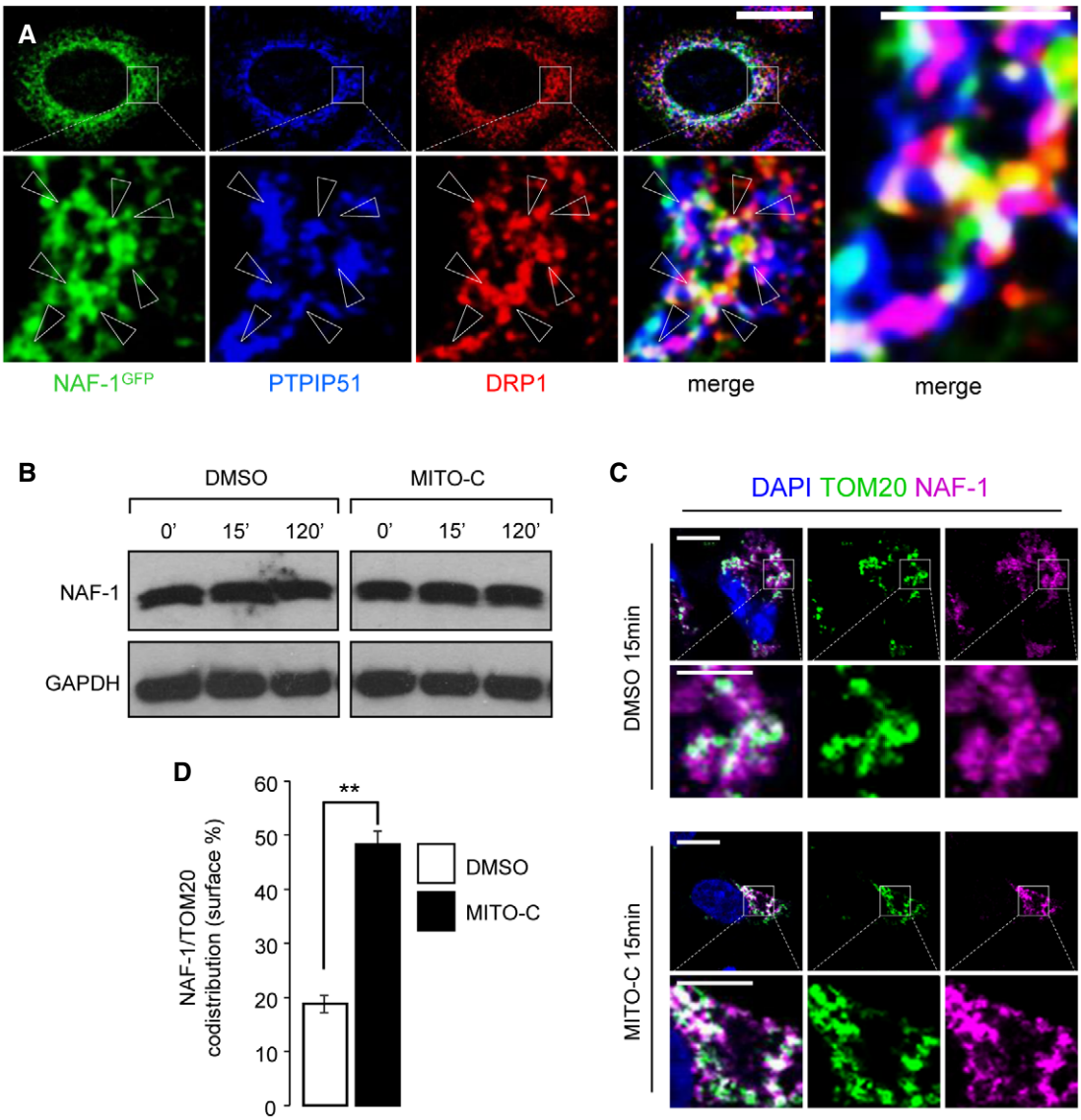

Figure EV4. MITO-C impact on NAF1 levels and subcellular localization.

A HeLa cells were transfected with NAF-1-GFP plasmid (green) and immunostained with antibodies to PTPIP51 (Blue) and DRP1 (red); three color merged image is shown in the far-right panel with arrowheads indicating the white triple colocalization domains.

B Western blot analysis of NAF-1 and GAPDH proteins expression in total extracts from HeLa cells treated with 2 μM Mito-C or DMSO for the indicated times.

C HeLa cells were treated with DMSO or 2 μM Mito-C for 15 min and immunostained with anti-TOM20 (green) and anti-NAF-1 (fuchsia) antibodies and DAPI (Blue).

D Quantification of NAF-1 signal on TOM20 positive structures. Errors bars show the standard error of the mean (SEM) (n = 75 cells from 3 independent experiments).

Data information: In D, one-way ANOVA followed by Dunn's post-test was used (** indicates $P < 0.005$). scale bars = 10 μm, except 4 μm in magnification area in A and in C.

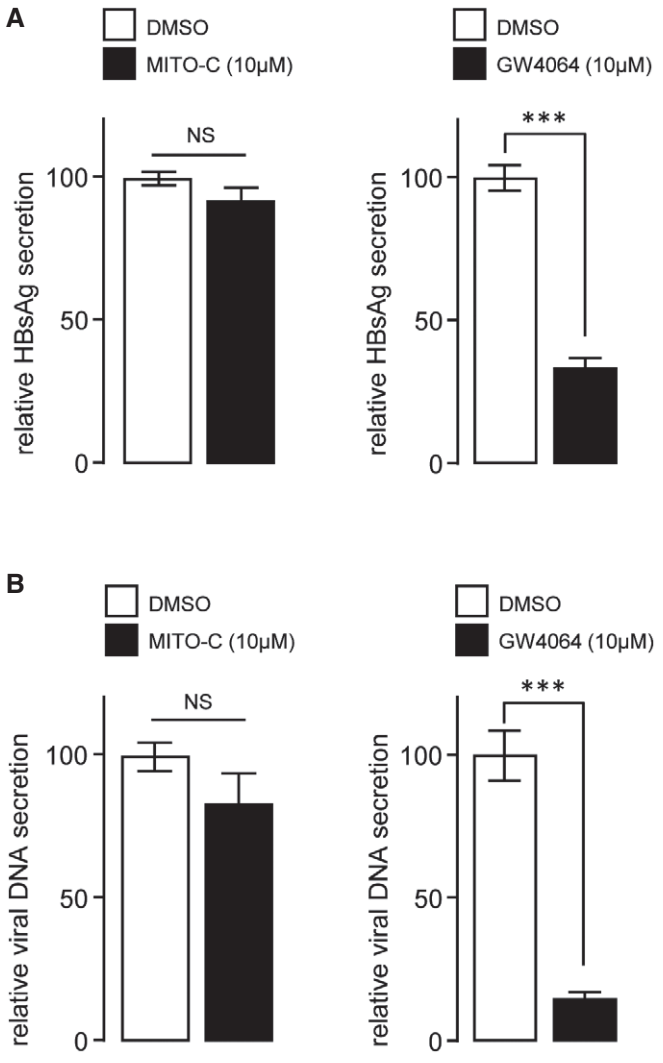

Figure EV5. Absence of MITO-C effect on Hepatitis B virus replication.

A Relative secretion of HBsAg (from Hepatitis B virus (HBV)) in dHepaRG cells treated post-infection with 10 μM of Mito-C or the FXR agonist GW4064. Bars show the standard deviation (SD) of 3 independent experiments.

B Relative secretion of HBV viral DNA in dHepaRG cells treated post-infection with 10 μM of Mito-C or GW4064 and quantified by quantitative PCR. Bars show the standard deviation (SD) of 3 independent experiments.

Data information: In A and B, one-way ANOVA followed by Dunn's post-test was used (*** indicates $P < 0.0001$).